Study of Gamma-Gamma Coincidence using Na^{22}

Aritra Mukhopadhyay

National Institute of Science Education and Research
Bhubaneswar, Odisha 751005, India
3rd year, Integrated M.Sc. Physics
Roll No.: 2011030
(Dated: January 29, 2023)

As the name implies, we examined and recorded the coincidences of gamma rays produced during the nuclear disintegration of the radioactive element Na^{22} in this experiment. We have measured and analysed the concurrent emission of gamma ray pairs produced in the positron-electron annihilation process using sodium iodide scintillators and specialised electronic modules. To demonstrate that the two annihilation gammas are not emitted 180 degrees in the lab frame in accordance with the principle of conservation of energy and momentum, coincidences are plotted and coincidence rates are calculated for different angles between the source and detector, such as $180°$, $175°$, $145°$ and $90°$. We find that the coincidences are maximum within a degree or less of $180°$ from one another.

I. THEORY

A. Annihilation Radiation

Coincidence refers to the simultaneous detection of the gamma that was released after the decay but in the opposite direction. The probability distribution for the decay of Na^{22} nuclei is 90% positron emission and 10% electron capture, as illustrated in the Fig 1.
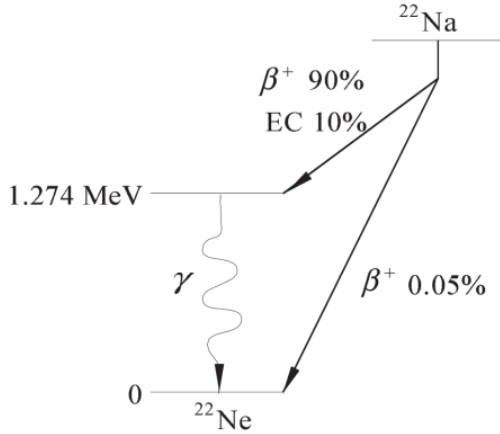

FIG. 1: **Decay of Na^{22}**

The ensuing Na^{22} nucleus deexcites to its ground state with the emission of a $1.274 MeV$ gamma ray with a mean lifetime of 3 picoseconds. Sodium Iodide scintillators and a photomultimeter are used to detect these gamma emissions. Using computer software, the output signal is amplified and presented as a histogram. The positrons are released with a variety of kinetic energy up to approximately a half mega electron volts, which they lose in the surrounding material at a rate of roughly one nanosecond, reducing to atomic energies in electron volts. To create positronium, a hydrogen-like "atom" with a lifespan of 10^-10s, they now catch an electron. This decay is caused by the annihilation of the positron and electron into two gammas.

Since the positron is at rest in its frame, the conservation of energy and momentum requires that the gamma be emitted in the opposite direction ($180°$) with equal kinetic energies, allowing for simultaneous detection in the detectors placed on both sides of the sample. Apiece gamma will have an energy $E_\gamma = 0.511\ MeV$ since the beginning energy of the positronium (ignoring the binding energy of a few eV) is only the rest mass energy of an electron and positron ($0.511 MeV$ each). However, the situation would be different in the laboratory frame, where the positronium will be moving with a range of kinetic energies up to a few eV. Then, depending on the direction of the initial positronium momentum relative to the gamma emission direction, the transformation to the lab frame gives gamma energies that might differ from $0.511\ MeV$ and/or produce gammas that are not emitted exactly $180°$ apart.

B. Experimental Setup

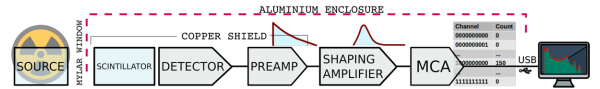The experimental setup is similar to that of Gamma ray spectroscopy and is shown in Fig 2.

FIG. 2: **Flow diagram for the entire process**

It is made up of a detector with an 8mm-diameter entrance window that is coated in aluminium to block out visible light. Inside, a semiconductor PN junction coupled in reverse bias mode is mated to a scintillator that measures 10mm by 10mm by 8mm. It is a Sodium Iodide scintillator with Thorium doping that emits photons with the same energy as the gamma ray's descent. The scintillation photons are transformed into an equivalent amount of electron-hole pairs in the depletion area of the PN junctions. An event in the photopeak area is

caused by the little amount of charge produced when one gamma ray deposits its whole energy in the scintillator and is subsequently transformed into a charge pulse by the PN junction. A charge sensitive preamplifier receives the charge pulse and converts it into a matching output voltage to produce a spectrum. The Shaping Amplifier then generates a pulse with a Guassian form. Depending on the amount of energy deposited, the amplitude ranges from 0 to 3.3 volts. The same buffered signal enters the built-in Multi-Channel Analyzer (MCA), whose hardware is capable of a number of tasks including pulse detection, post-processing, and sorting signals based on peak height into predefined bins with a 10bit resolution. The input voltage range for the MCA is 0 to 3.3V. The programme CNSPEC includes a wide range of tools for data analysis and can plot the obtained data in real-time.

C. Coincidence Rate

The nuclear decay rate (number of nuclear decays per second) is $\tau_n = \alpha 3.7 \times 10^{10} decays/sec/curie$, where α is the source activity in curies. For the 90% probability of gamma emission, the rate of emission of 0.511 MeV gammas is 1.8 τ_n. These gammas are emitted uniformly (in oppositely directed pairs) from the source. Thus at a distance R from the source they are spread out over an area $4\pi R^2$ and the flux ϕ (number per unit area per second) will be:

$$\phi = 1.8\tau_n 4\pi R^2$$

The apertures, the scintillators and their relationship to the source and each other are an important factor in determining the rates at which gammas are detected. The fraction of 0.511 MeV gammas which get through the lead shielding will also need to be specified. It is expected to be on the order of 20% and will be expressed by the symbol κ.

With these considerations, the rate Q of 0.511 MeV gammas striking the face of the scintillator can be calculated.

$$Q = \phi[A_a + \kappa(A_s - A_a)]$$

where the area of the aperture is $A_a = \pi r_a^2$, and the area of the scintillator is $A_s = \pi r_s^2$, where r_i are the respective radii.

II. OBSERVATIONS

A. 180 degree Data

In figure Fig 3 we can see the calibration information for mapping the channels to appropriate enrgies. In Fig 4 and Fig 5 we can see the coincident counts from the

two sensors. Finally in Fig 6 we can see the analysis data about the observation.
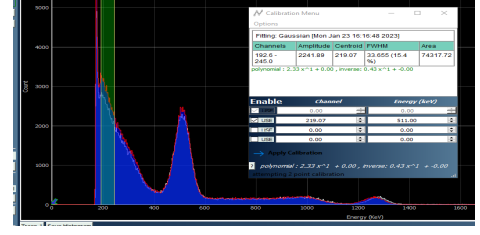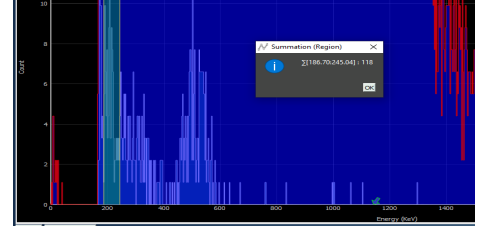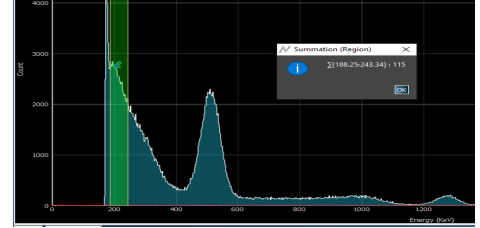

FIG. 3: 180° calibration

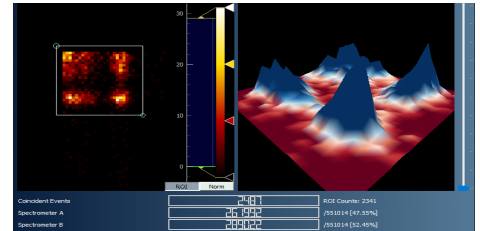FIG. 4: 180° blue count

FIG. 5: 180° red count

FIG. 6: 180° analysis

B. 175 degree Data

In figure Fig 7 we can see the calibration information for mapping the channels to appropriate enrgies. In Fig 8 and Fig 9 we can see the coincident counts from the two sensors. Finally in Fig 10 we can see the analysis data about the observation.
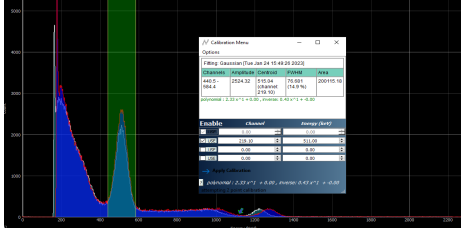
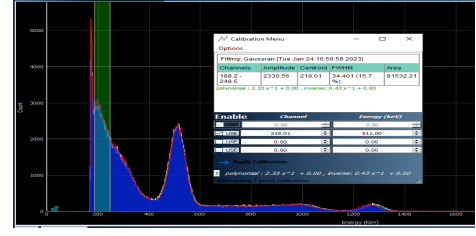FIG. 7: 175° calibration

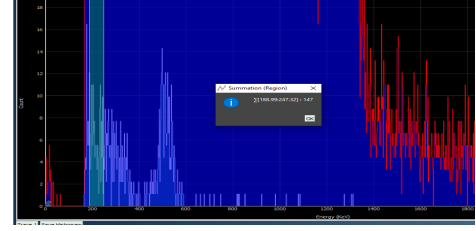FIG. 11: 185° calibration

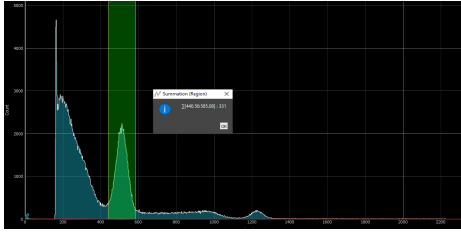FIG. 8: 175° blue count

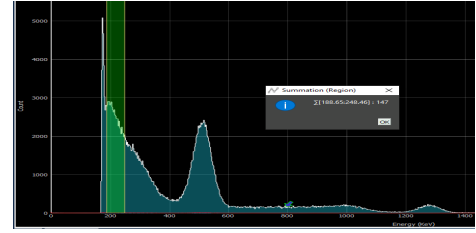FIG. 12: 185° blue count

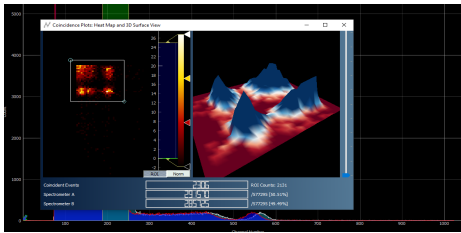FIG. 9: 175° red count

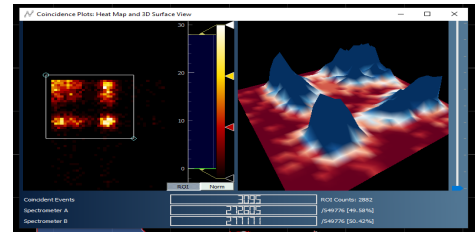FIG. 13: 185° red count

FIG. 10: 175° analysis

FIG. 14: 185° analysis

C. 185 degree Data

In figure Fig 11 we can see the calibration information for mapping the channels to appropriate enrgies. In Fig 12 and Fig 13 we can see the coincident counts from the two sensors. Finally in Fig 14 we can see the analysis data about the observation.

D. 90 degree Data

In figure Fig 15 we can see the calibration information for mapping the channels to appropriate enrgies. In Fig 16 and Fig 17 we can see the coincident counts from the two sensors. Finally in Fig 18 we can see the analysis data about the observation.
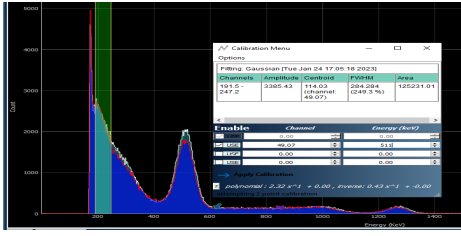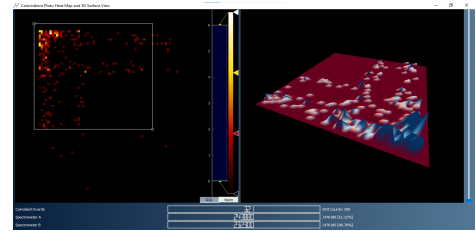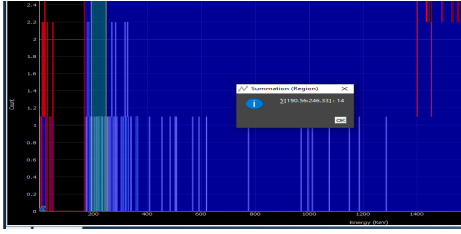
FIG. 15: 90° calibration
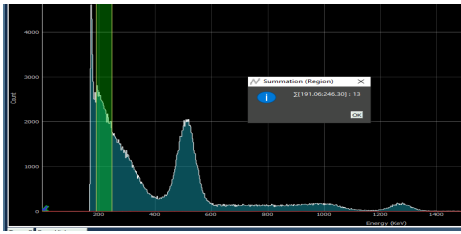

FIG. 18: 90° analysis

FIG. 16: 90° blue count

FIG. 17: 90° red count